

Research Paper

Facile Synthesis and Potential Bioimaging Applications of Hybrid Upconverting and Plasmonic NaGdF₄: Yb³⁺, Er³⁺/Silica/Gold Nanoparticles

Sha Liu^{1,2}, Guanying Chen¹, Tymish Y. Ohulchanskyy¹, Mark T. Swihart^{1,2}✉, and Paras N. Prasad¹✉

1. Institute for Lasers, Photonics and Biophotonics, University at Buffalo, The State University of New York, Buffalo, New York 14260, United States;
2. Department of Chemical and Biological Engineering, University at Buffalo, The State University of New York, Buffalo, New York 14260, United States.

✉ Corresponding author: pnprasad@buffalo.edu or swihart@buffalo.edu.

© Ivyspring International Publisher. This is an open-access article distributed under the terms of the Creative Commons License (<http://creativecommons.org/licenses/by-nc-nd/3.0/>). Reproduction is permitted for personal, noncommercial use, provided that the article is in whole, unmodified, and properly cited.

Received: 2012.08.04; Accepted: 2012.09.23; Published: 2013.03.21

Abstract

We present a simple method for preparing water dispersible NaGdF₄: Yb³⁺, Er³⁺/silica/gold nanoparticles. The emission intensity and color of the upconverting cores are modulated by the plasmonic absorbance and field enhancement from the gold nanoparticles. The applicability of hybrid NPs for multi-modal bioimaging probes is illustrated by *in vitro* confocal microscopy of living cancer cells.

Key words: Upconversion, Gold, Nanoparticles, Photoluminescence, Bioimaging.

1. Introduction

Hybrid nanoparticles are of great interest because of their potential to combine desirable properties of different nanostructures in a single construct[1]. They have potential applications in multi-modal bioimaging[2, 3], diagnostics, and therapy[4, 5] as well as in photonics and optoelectronics. Lanthanide-doped upconversion (UC) nanophosphors are promising optical contrast agents for biomedical applications due to their photostability, sharp emission peaks, and long emission lifetime[6, 7]. Upon near infrared (NIR) excitation, UC nanoparticles exhibit intense visible emission via multiphoton processes involving the lanthanide ions within them[8-10]. For *in vitro* or *in vivo* imaging, the use of NIR excitation minimizes absorbance, scattering, and fluorescence from cells and tissues, allowing imaging against a dark background[11]. In contrast, commercially available labels, such as organic dyes and quantum dots, typically must be imaged against a

background of Stokes-shifted tissue auto-fluorescence induced by UV, blue, or green excitation[12]. In addition, because of the existence of real intermediate energy levels in lanthanide ions, this upconversion process can be much more efficient than conventional multiphoton-absorption-induced fluorescence of organic dyes or quantum dots, where the intermediate levels are virtual. This high efficiency enables the use of low-cost, CW, NIR diode lasers as excitation sources, rather than the expensive and complex femtosecond laser sources required for conventional multiphoton fluorescence of organic dyes and quantum dots[13].

Judiciously combining these UC nanoparticles (NPs) with other nanostructures may enable even greater control of their optical properties or generation of entirely new combinations of properties not available in single-component nanoparticles[14]. Au NPs have potential applications in thermal thera-

py[15], bioimaging[16], photosensing[17], and other imaging and therapeutic technologies based on their strong surface plasmon resonance absorption[18] and scattering. Integration of Au NPs with UC NPs could provide enhancement of UC emission, due to local field enhancement by the Au NPs, or could provide attenuation of UC emission via energy transfer from the UC NPs to the Au NPs[1, 19]. Understanding and harnessing these interactions are of both scientific and practical interest. NaGdF₄ provides one of the best host lattices for creating lanthanide-doped UC NPs[20, 21]. Moreover, NaGdF₄ NPs have been demonstrated as magnetic resonance imaging contrast agents, using positive-contrast enhancement[22-24] which opens the door to multimodal imaging using Gd-containing UC NPs[25]. In this communication, we report a simple method to prepare water-dispersible hybrid nanoparticles of NaGdF₄: Er,Yb (UC NPs) and gold NPs. The hybrid particles combine the magnetic and optical properties of the Gd-based UC NPs and surface plasmon resonance of gold NPs, and have potential applications in the fields of bioimaging[26], MRI and thermal therapy.

Very recently, as we were drafting this manuscript, Li *et al.*[27] published a similar method for synthesizing hybrids of 20 nm diameter NaYF₄:Yb/Er nanophosphors and gold nanoparticles for use in biosensors. However, we present here a hybrid nanostructure of 10 nm diameter NaGdF₄:Yb/Er nanophosphors and gold nanoparticles for their applications in multi-modal bioimaging. Although MRI is not an explicit focus of this paper, the known effectiveness of these Gd-containing nanoparticles as MRI contrast agents provides these particles with potential for multimodal (MRI plus optical) imaging for which the NaYF₄ based particles could not be used.

2. Experimental Section

2.1 Synthesis of β -NaGdF₄:Yb20%Er2% Nanocrystals

0.39 mmol gadolinium(III) chloride hexahydrate (GdCl₃·6H₂O, Aldrich, 99.999%), 0.1 mmol ytterbium(III) chloride hexahydrate (YbCl₃·6H₂O, Aldrich), and 0.01 mmol erbium chloride hexahydrate (ErCl₃·6H₂O, Aldrich, 99.9%) were added to a 100 mL three-neck round-bottom flask. Then 4 mL oleic acid (Aldrich, 90%) and 16 mL 1-octadecene (Aldrich, 90%) were added. The flask was heated to 160 °C under argon gas flow with constant stirring for 2 hours, and then cooled to room temperature. 1.8 mmol ammonium fluoride (NH₄F, sigma-Aldrich) and 1.25 mmol sodium hydroxide (NaOH, Sigma-Aldrich) dissolved in

methanol (Fisher) were added, and the mixture was stirred at 50 °C for 30 min. After the methanol had evaporated, the solution was heated to 300 °C as quickly as possible under argon gas flow with vigorous stirring, held at that temperature for 60 min, and then cooled to room temperature. The obtained nanoparticles were precipitated by the addition of 15 mL acetone, collected by centrifugation at 11000 rpm for 10 min, washed with ethanol several times, and finally dispersed in 10 mL cyclohexane (Sigma-Aldrich, 99%).

2.2 Synthesis of 5 nm PVP capped-gold nanoparticles

0.16 mL of gold chloride trihydrate (HAuCl₄, Aldrich, 99%) aqueous solution (5 mM) was diluted with 2 mL DI water and then 2 mL of 7 mg/mL polyvinylpyrrolidone (PVP, Aldrich, M.W. 40,000) in water was added. After 30 min of stirring, 200 μ L of 0.1 M NaBH₄ aqueous solution was added. After several minutes, the color of the solution changed to red indicating gold NP formation. The synthesized particles were used in further experiments without washing

2.3 Coating upconverting particles with silica shell

0.35 mL Igepal CO-520 (Aldrich) was mixed with 6 mL cyclohexane, and then 0.5 mL of a 100 mM (concentration of Gd³⁺) dispersion of upconverting particles was added. After 30 min stirring, 200 μ L ammonium hydroxide (Sigma-Aldrich, 28%-30%) was added and the stirring was maintained for another 1 hour until the solution became clear. 40 μ L tetraethylorthosilicate (TEOS, Aldrich, 97%) was then added, and the solution was stirred overnight. The synthesized particles were precipitated with acetone and then collected by centrifugation at 8000 rpm for 10 min. 6 mL DI water was used to redisperse particles for further experiments.

2.4 APTES functionalized NaGdF₄:Yb, Er/silica

3 mL of 12 mM 3-aminopropyltriethoxysilane (APTES, Aldrich, 99%) in ethanol was added to the NaGdF₄:Yb, Er/silica nanoparticles from the previous step, and then the solution was refluxed at 80 °C for 1 hour. Functionalized particles were centrifuged out at 8000 rpm and were further washed with a mixture of DI water and ethanol. Finally, the obtained particles were dispersed in 2 mL ethanol.

2.5 Gold nanoparticle attachment to NaGdF₄:Yb, Er/silica

2 mL ethanol solution of NaGdF₄:Yb, Er/silica nanoparticles was mixed with another 2 mL ethanol

and then 1.5 mL water solution of synthesized gold nanoparticles was added with stirring. After 1 hour, particles were centrifuged out, and then redispersed either in ethanol or water for further characterization.

2.6 Cellular imaging

For in vitro imaging, HeLa cells were cultured in Dulbecco's minimum essential medium (DMEM) with 10% fetal bovine serum (FBS), 1% penicillin, and 1% amphotericin B. The day before nanoparticle treatment, cells were seeded in 35 mm culture dishes. On the treatment day, the cells, at a confluency of 50–60%, in serum-supplemented medium, were treated with the nanoparticles at a specific concentration (100 μ L per 1 mL of medium) and incubated overnight at 37 °C. After incubation, the cells were rinsed with the medium once.

Confocal microscopy images were obtained using a Leica TCS SP2 AOBS spectral confocal microscope (Leica Microsystems Semiconductor GmbH, Wetzlar, Germany) with laser excitation at 514 nm (reflection and transmission images) or 975 nm (UC luminescence image).

2.7. Instruments

The size and morphology of gold and UC nanocrystals were characterized by transmission electron microscopy using a JEOL JEM-2010 microscope at an acceleration voltage of 200 kV. Absorption spectra were acquired using a Shimadzu 3600 UV-Visible-NIR scanning spectrophotometer. The UC emission spectra were obtained using a Fluorolog-3.11 spectrofluorometer (Jobin Yvon) under excitation at 975 nm using a fiber-coupled laser diode (Q-Photonics). The decay profiles were recorded by an Infinium oscilloscope (Hewlett-Packard) coupled to the output of the photomultiplier tube (PMT) of the Fluorolog-3.11 spectrofluorimeter, using laser diode excitation at 975 nm operating in the pulsed mode (pulse width of 300 μ s) at 400 Hz. Samples with and without addition of Au NPs were measured under identical conditions and at the same concentration. To achieve this, two samples were taken from a given batch of silica-coated NPs. Au NPs were added to one sample, while the other was retained for comparison. If some UC NPs were lost during centrifugation and re-dispersion after Au NP addition, then the concentration of the sample with Au NPs could be slightly lower than that without Au NP addition.

3. Results and Discussion

Direct growth of gold NPs on UC NPs was not successful, because homogeneous nucleation of Au NPs is favored over heterogeneous nucleation of Au

on the UC NPs under all conditions we have explored. Moreover, direct, intimate contact between the UC NPs and Au NPs may not be desirable, as it could lead to complete quenching of UC NP emission. Therefore, a simple method was designed here for decorating UC NPs with gold NPs and simultaneously transferring the hydrophobic UC NPs to an aqueous environment. The overall approach is illustrated schematically in figure 1, and described in greater detail in the experimental section. Monodispersed UC NaGdF₄:2% Er, 20% Yb NPs capped by oleic acid were first synthesized via a procedure adapted from our recent work[24]. The hydrophobic UC NPs were then capped with silica via a reverse-micelle method[28] to make them hydrophilic. Amino-propyltriethoxysilane (APTES) was then used to functionalize the silica-capped UC NPs with amine groups. Finally, 5 nm gold NPs capped with PVP were mixed with the silica-coated UC NPs. Amine groups on the UC NPs displaced the PVP from the AuNP surface, yielding AuNP-decorated UC NPs that were dispersible in water or ethanol.

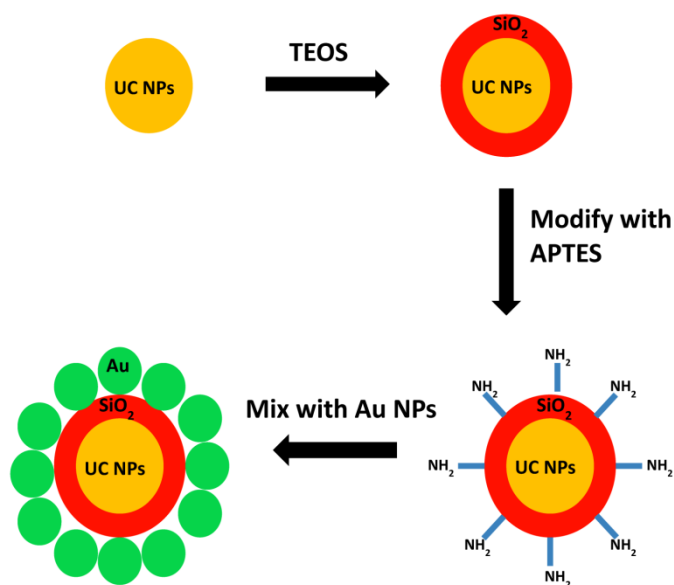


Figure 1. Schematic illustration of synthetic procedures.

The NaGdF₄: Er, Yb particles have hexagonal crystal structure, as demonstrated by selected area electron diffraction (figure 2(a)), which typically leads to higher quantum yield than the cubic phase[29]. TEM images (figure 3), show that the UC NPs have a mean diameter of about 10 nm, and the thickness of the silica shell is about 6 nm, yielding an overall diameter near 22 nm for the coated particles. Figure 3(b) shows the size of UC NPs/silica core-shell particles and their mono-dispersity. Figure 3(c) and (d) show

the hybrid particles following the attachment of 5 nm Au NPs. After the UC NPs were decorated with Au NPs, the dispersion turned red. Figure 2(b) shows the extinction spectrum of the NaGdF₄:Er,Yb/silica/AuNP dispersion in water, with a peak near 530 nm, attributed to the plasmon resonance absorbance and scattering by Au NPs.

Figure 4(a) shows the emission spectra of the hybrid particles under 975 nm excitation. Two UC bands with maxima at 520/540 nm and 650 nm are seen, corresponding to the $^2H_{11/2}/^4S_{3/2} \rightarrow ^4I_{15/2}$ and $^4F_{9/2} \rightarrow ^4I_{15/2}$ transitions (of Er³⁺), respectively. The up-conversion mechanisms are shown schematically in figure 5. The 975 nm laser excites Yb³⁺ ions from the ground state to the $^2F_{5/2}$ state. Then, two discrete energy transfers from the excited Yb³⁺ ions bring the Er³⁺ ions from the ground state to the $^2H_{11/2}/^4S_{3/2}$ states, which produces UC emission at 520/540 nm by radiative decay to the ground $^4I_{15/2}$ state. The red UC emission at 650 nm arises from the $^4F_{9/2}$ state, which can be populated by either nonradiative decay from the $^2H_{11/2}/^4S_{3/2}$ state or by exciting Er³⁺ ions from the $^4I_{13/2}$ state to the $^4F_{9/2}$ state through energy transfer from Yb³⁺ ions.

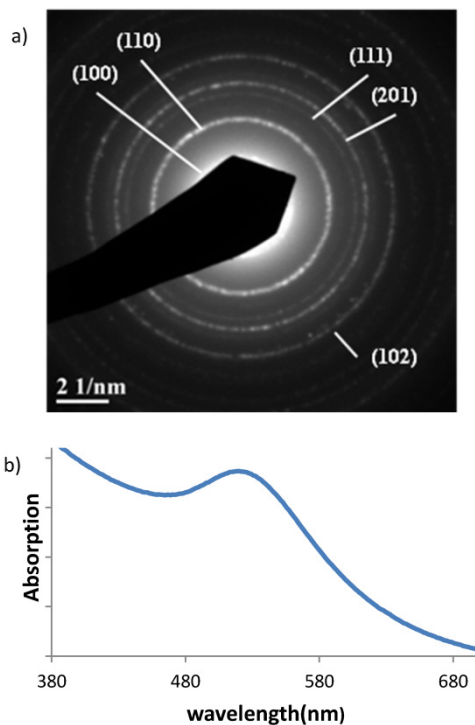


Figure 2. (a) Selected area electron diffraction image of NaGdF₄:Er³⁺,Yb³⁺ nanocrystals. (b) Absorption spectrum of NaGdF₄:Er³⁺,Yb³⁺/silica/AuNP water dispersion.

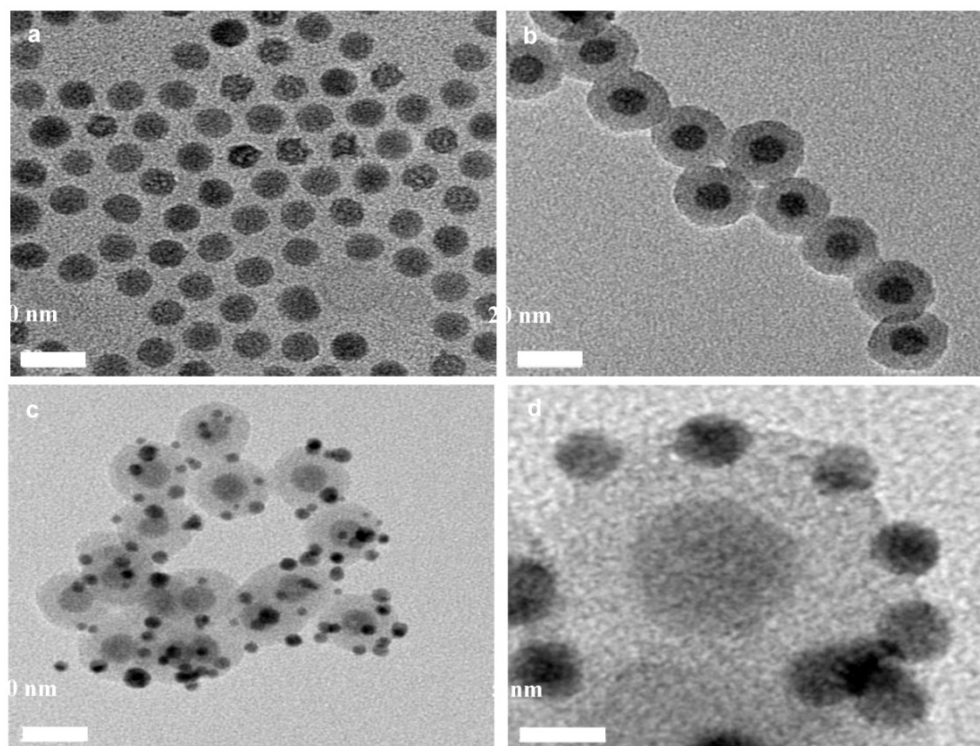


Figure 3. TEM images of (a) UC NPs; (b) UC/silica NPs; (c) UC/silica/Au NPs; (d) higher magnification of UC/silica/Au NPs.

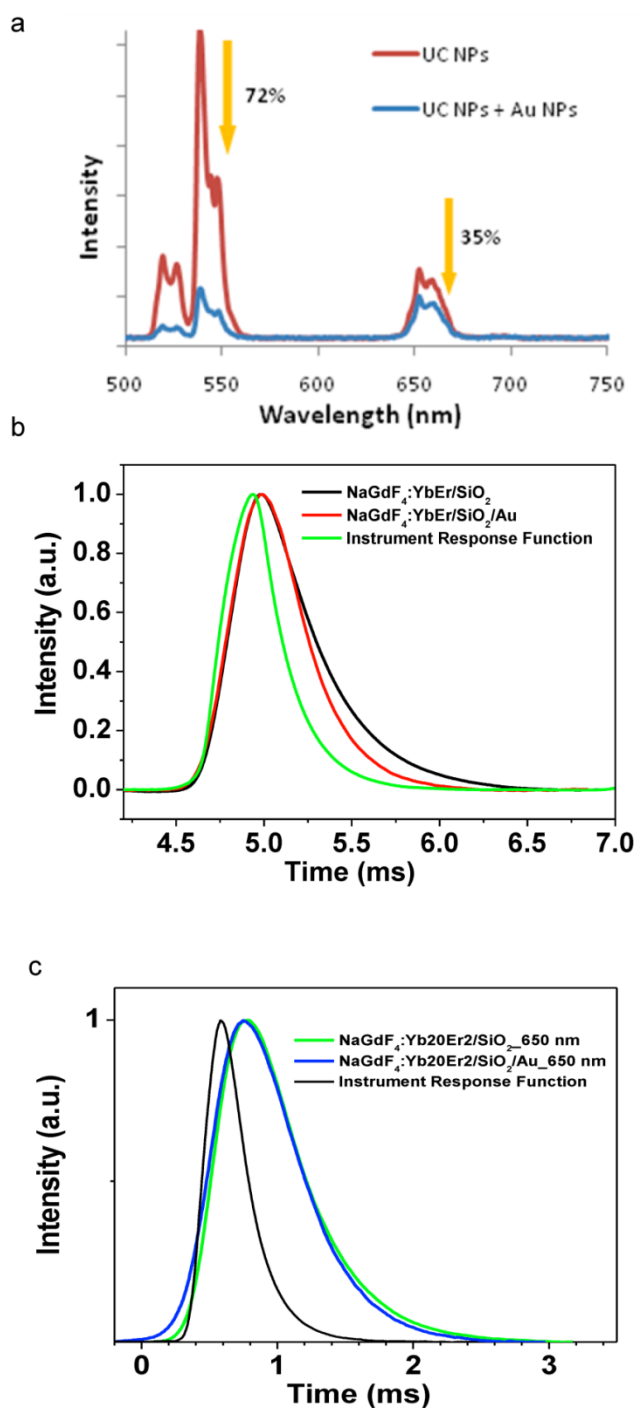


Figure 4. Photoluminescence spectra (a) and lifetime (b) of green emission for UC NPs before and after decorating with Au NPs. (c) Decay of red emission for UC NPs before and after decorating with Au NPs. Spectra presented in part (a) were measured under identical conditions and NP concentration.

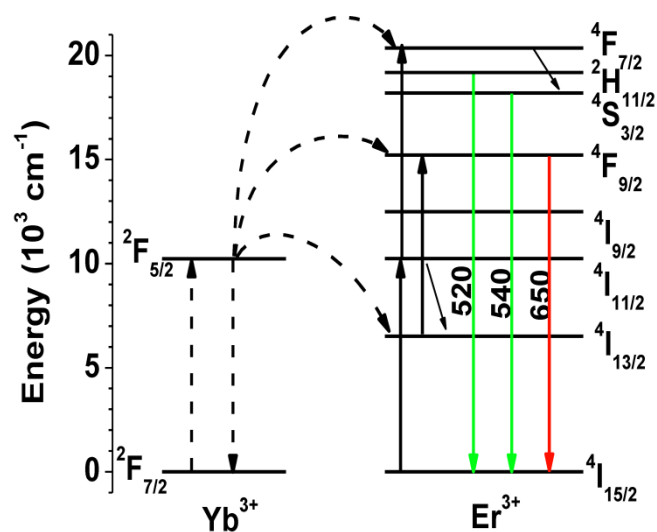


Figure 5. Energy level diagrams of Yb^{3+} and Er^{3+} ions and the proposed upconversion mechanism in $\text{NaGdF}_4: \text{Yb}^{3+}, \text{Er}^{3+}$ nanocrystals

Upon decoration with Au NPs, the relative UC emission intensities of the hybrid NPs was modulated dramatically, as shown in figure 4 (a). The intensity of the green emission peak at 520/540 nm was reduced by 72% after Au NP addition, while the red emission near 650 nm was attenuated by only 35%. The difference in attenuation for the two bands demonstrates the utility of plasmonic particles for tuning UC colors, which is potentially useful in creating bio-sensors[27]. The surface plasmon resonance of gold can also affect the emission intensities of luminescent particles by shortening the luminescence lifetime[30]. To further clarify this effect, we measured the decay of the green emission at 540 nm. As illustrated in figure 4(b), the lifetime of the green emission was decreased from $\sim 300 \mu\text{s}$ to $\sim 200 \mu\text{s}$. The lifetime of the red emission at 650 nm appeared to be almost unchanged under these conditions (figure 4(c)), but it noticeably decreased for a sample with a higher concentration of gold nanoparticles. The different lifetime shortening for the green and the red emissions is apparently induced by Au NPs and associated with energy transfer to the gold nanoparticles[31]. If the lifetime shortening was due to increased radiative deactivation rate, then we would expect enhancement of UC emission intensity[30]. However, a decreased intensity was observed for both emission bands. Energy transfer from the UC NP to the Au NP at 520/540 nm could provide a parallel, nonradiative pathway that would compete with the radiative one and decrease the emission intensity. However, a parallel nonradiative path that decreased the lifetime by only 30% would also only decrease the total emission intensity by about 30%. Thus, the direct

energy transfer may contribute to the intensity decrease, but does not appear to be the dominant effect. Finally, the emission intensity can also be decreased due to absorption of the emitted light by the Au NPs, without affecting the emission lifetime. All of these effects: enhancement of radiative recombination rate, direct energy transfer (non-radiative rate), and Au reabsorption are expected to be strongest for the green emission band that overlaps with the plasmon resonance of the gold nanoparticles. Therefore, the intensity of this band decreased more than that of the band peaked at 650 nm. Some researchers have observed an increase in photoluminescence of upconverting NPs upon encapsulation with a gold shell. However, others have shown that a decrease in photoluminescence is also possible. Multiple factors may affect the interaction between gold and upconverting NPs, including the distance between gold and upconverting NPs, the ratio of gold NPs to UC NPs, and the surfactants used. These factors will affect both radiative and non-radiative pathways, such that different combinations may lead to either a net enhancement or net attenuation of luminescence.

The water-dispersible hybrid nanoparticles possess both plasmonic and UC photoluminescence properties, which can be exploited for bioimaging.

Figure 6 illustrates the bimodal imaging capability of the NaGdF₄:Er,Yb/silica/Au NPs. HeLa cells were incubated with these nanoparticles overnight at 37 °C, rinsed, and imaged with a confocal microscope. Plasmonic properties of the nanoparticles taken up by cells produce strong contrast in confocal reflection imaging using the 514 nm laser excitation (figure 6b) because of the strong scattering from gold particles. On the other hand, due to the photoluminescence of UC nanoparticle cores, the luminescence cellular imaging can also be obtained when excited at 975 nm (figure 6c). As bioimaging probes, upconversion nanoparticles would be more valuable if their emission efficiency were higher, comparable to that of quantum dots. The doping of gold nanoparticles has been shown in this paper to tune the emission intensity of UC nanoparticles. In the future, the distance between gold and UC nanoparticles and the ratio between them can be controlled to optimize the surface plasmon enhancement effect of gold nanoparticles to increase the emission intensity of UC nanoparticles and further increase the photoluminescence efficiency. Moreover, the Gd-containing host material makes these materials relevant to MRI contrast enhancement as well. This possibility should be investigated further in the future.

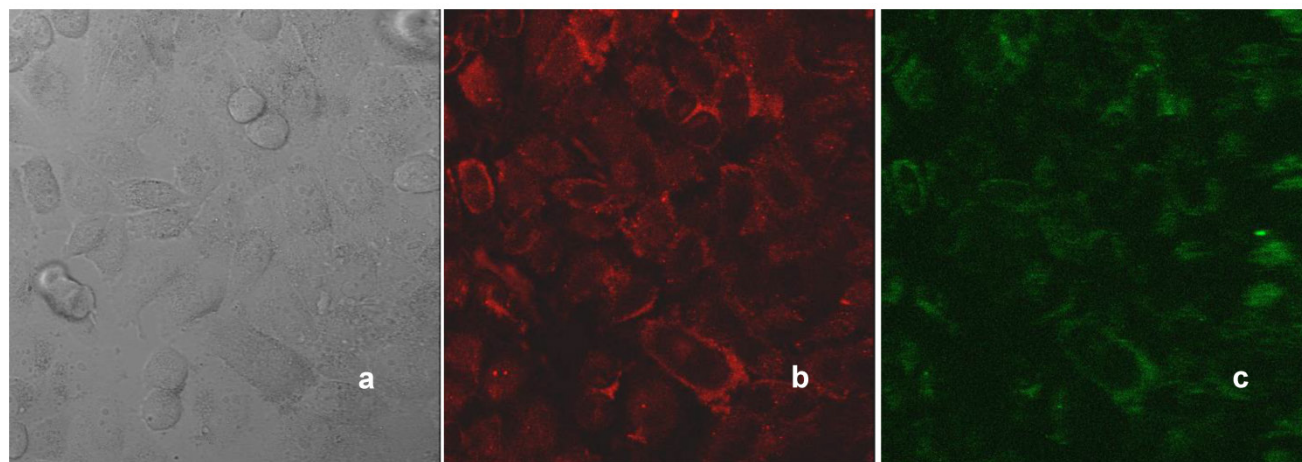


Figure 6. Confocal microscopy images of HeLa cells treated with NaGdF₄:Er,Yb/silica/Au nanoparticles: (a) transmission; (b) reflection (514 nm laser line); (c) UC photoluminescence (975 nm excitation, detection in the range of 500-700 nm).

4. Conclusion

In summary, water dispersible NaGdF₄:Er³⁺, Yb³⁺/silica/Au NPs with overall diameters around 20 nm have been prepared. The color and the intensity of UC emission under NIR excitation at 975 nm were changed by the gold NPs. This can be attributed primarily to the surface plasmon resonance absorption by gold nanoparticles. The lifetime of the UC emission

was found to decrease slightly as a result of interaction with the gold nanoparticles, suggesting the possibility of non-radiative energy transfer from the UC NPs to Au NPs and/or increase in the rate of radiative deactivation. UC photoluminescence and confocal reflection imaging demonstrated uptake of hybrid nanoparticles by cancer cells *in vitro* and the possibility of dual modality imaging exploiting both the plasmonic and the UC photoluminescent properties of

the NaGdF₄:Er,Yb/silica/Au NPs. Though not demonstrated here, MRI contrast enhancement by Gd is expected to enable a third imaging modality. Plasmonic effects on UC NPs depend strongly on the size of gold NPs and the distance between UC NPs and the gold NPs. Future fine tuning of these parameters might result in other interesting phenomena, such as emission enhancement, emission color change, and emission lifetime modulation.

Acknowledgement

This work was supported in part by grants from the National Institutes of Health (R01CA119358 and R01CA104492) and by the University at Buffalo Integrated Nanostructured Systems Instrument Facility. We are grateful to Mark Kaus for assistance in synthesizing Au NPs.

Competing Interests

The authors have declared that no competing interest exists.

References

- Wang LY, Yan RX, Hao ZY, Wang L, Zeng JH, Bao H, Wang X, Peng Q, and Li YD. Fluorescence resonant energy transfer biosensor based on upconversion-luminescent nanoparticles. *Angewandte Chemie-International Edition*. 2005; 44(37): 6054-6057.
- Yi DK, Selvan ST, Lee SS, Papaefthymiou GC, Kundaliya D, and Ying JY. Silica-Coated Nanocomposites of Magnetic Nanoparticles and Quantum Dots. *Journal of the American Chemical Society*. 2005; 127(14): 4990-4991.
- Chen D, Yu Y, Huang F, Yang A, and Wang Y. Lanthanide activator doped NaYb_{1-x}Gd_xF₄ nanocrystals with tunable down-, up-conversion luminescence and paramagnetic properties. *Journal of Materials Chemistry*. 2011; 21(17): 6186-6192.
- Sokolov K, Larson TA, Bankson J, and Aaron J. Hybrid plasmonic magnetic nanoparticles as molecular specific agents for MRI/optical imaging and photothermal therapy of cancer cells. *Nanotechnology*. 2007; 18(32):325101.
- Yu MK, Park J, and Jon S. Targeting Strategies for Multifunctional Nanoparticles in Cancer Imaging and Therapy. *Theranostics*. 2012; 2(1):3-44.
- Wu SW, Han G, Milliron DJ, Aloni S, Altoe V, Talapin DV, Cohen BE, and Schuck PJ. Non-blinking and photostable upconverted luminescence from single lanthanide-doped nanocrystals. *Proceedings of the National Academy of Sciences of the United States of America*. 2009; 106(27): 10917-10921.
- Mai HX, Zhang YW, Si R, Yan ZG, Sun Ld, You LP, and Yan CH. High-Quality Sodium Rare-Earth Fluoride Nanocrystals: Controlled Synthesis and Optical Properties. *J. Am. Chem. Soc.* 2006; 128(19): 6426-6436.
- Boyer JC, Cuccia LA, and Capobianco JA. Synthesis of Colloidal Upconverting NaYF₄: Er³⁺/Yb³⁺ and Tm³⁺/Yb³⁺ Monodisperse Nanocrystals. *Nano Letters*. 2007; 7(3):847-852.
- Heer S, Kömpe K, Güdel HU, and Haase M. Highly Efficient Multicolour Upconversion Emission in Transparent Colloids of Lanthanide-Doped NaYF₄ Nanocrystals. *Advanced Materials*. 2004; 16(23-24):2102-2105.
- Chen GY, Ohulchanskyy T, Kumar R, Agren H, and Prasad PN. Ultrasmall Monodisperse NaYF₄:Yb³⁺/Tm³⁺ Nanocrystals with Enhanced Near-Infrared to Near-Infrared Upconversion Photoluminescence. *ACS Nano*. 2010; 4(6):3163-3168.
- Nyk M, Kumar R, Ohulchanskyy TY, Bergey EJ, and Prasad PN. High Contrast in Vitro and in Vivo Photoluminescence Bioimaging Using Near Infrared to Near Infrared Up-Conversion in Tm³⁺ and Yb³⁺ Doped Fluoride Nanophosphors. *Nano Letters*. 2008; 8(11):3834-3838.
- Wang M, Mi CC, Wang WX, Liu CH, Wu YF, Xu ZR, Mao CB, and Xu SK. Immunolabeling and NIR-Excited Fluorescent Imaging of HeLa Cells by Using NaYF₄:Yb,Er Upconversion Nanoparticles. *ACS Nano*. 2009; 3(6):1580-1586.
- Prasad PN. *Introduction to Biophotonics*. New York: Wiley-Interscience. 2003.
- Chen D, Lei L, Yang A, Wang Z, and Wang Y. Ultra-broadband near-infrared excitable upconversion core/shell nanocrystals. *Chemical Communications*. 2012; 48(47):5898-5900.
- O'Neal DP, Hirsch LR, Halas NJ, Payne JD, and West JL. Photo-thermal tumor ablation in mice using near infrared-absorbing nanoparticles. *Cancer Letters*. 2004; 209(2):171-176.
- Sharma P, Brown S, Walter G, Santra S, and Moudgil B. Nanoparticles for bioimaging. *Advances in Colloid and Interface Science*. 2006; 123:471-485.
- Jang B and Choi Y. Photosensitizer-Conjugated Gold Nanorods for Enzyme-Activatable Fluorescence Imaging and Photodynamic Therapy. *Theranostics*. 2012; 2(2):190.
- Liu S, Chen G, Prasad PN, and Swihart MT. Synthesis of Monodisperse Au, Ag, and Au-Ag Alloy Nanoparticles with Tunable Size and Surface Plasmon Resonance Frequency. *Chemistry of Materials*. 2011; 23(18): 4098.
- Kondo M, Uchikawa M, Kume S, and Nishihara H. Alcohol- and acid-causing reversible switching of near-infrared absorption and luminescence in a donor-acceptor conjugated system. *Chemical Communications*. 2009; 15:1993-1995.
- Liu YS, Tu DT, Zhu HM, Li R., Luo WQ, and Chen XY. A Strategy to Achieve Efficient Dual-Mode Luminescence of Eu³⁺ in Lanthanides Doped Multifunctional NaGdF₄ Nanocrystals. *Advanced Materials*. 2010; 22(30):3266-3271.
- Wang F, Wang JA and Liu XG. Direct Evidence of a Surface Quenching Effect on Size-Dependent Luminescence of Upconversion Nanoparticles. *Angewandte Chemie-International Edition*. 2010; 49(41): 7456-7460.
- Abel KA, Boyer JC, and Veggel FCJMv. Hard Proof of the NaYF₄/NaGdF₄ Nanocrystal Core/Shell Structure. *Journal of the American Chemical Society*. 2009; 131(41):14644-14645.
- Zhen Z and Xie J. Development of Manganese-Based Nanoparticles as Contrast Probes for Magnetic Resonance Imaging. *Theranostics*. 2012; 2(1):45-54.
- Chen GY, Ohulchanskyy TY, Law WC, Agren, H., and Prasad, P.N., Monodisperse NaYbF₄: Tm³⁺/NaGdF₄ core/shell nanocrystals with near-infrared to near-infrared upconversion photoluminescence and magnetic resonance properties. *Nanoscale*. 2011; 3: 2003-2008.
- Kumar R, Nyk M, Ohulchanskyy TY, Flask CA, and Prasad PN. Combined Optical and MR Bioimaging Using Rare Earth Ion Doped NaYF₄ Nanocrystals. *Advanced Functional Materials*. 2009; 19(6):853-859.
- Xing H, Bu W, Zhang S, Zheng X, Li M, Chen F, He, Q., Zhou, L., Peng, W., Hua, Y., and Shi, J., Multifunctional nanoprobe for upconversion fluorescence, MR and CT trimodal imaging. *Biomaterials*. 2012;33(4):1079-1089.
- Li Z, Wang L, Wang Z, Liu X, and Xiong Y. Modification of NaYF₄:Yb,Er@SiO₂ Nanoparticles with Gold Nanocrystals for Tunable Green-to-Red Upconversion Emissions. *The Journal of Physical Chemistry C*. 2011;115(8):3291-3296.
- Han Y, Jiang J, Lee SS, and Ying JY. Reverse Microemulsion-Mediated Synthesis of Silica-Coated Gold and Silver Nanoparticles. *Langmuir*. 2008; 24(11):5842-5848.
- Krämer KW, Biner D, Frei G, Güdel, H.U., Hehlen, M.P., and Lüthi, S.R., Hexagonal Sodium Yttrium Fluoride Based Green and Blue Emitting Upconversion Phosphors. *Chemistry of Materials*. 2004; 16(7):1244-1251.
- Zhang H, Li YJ, Ivanov IA, Qu YQ, Huang Y, and Duan XF. Plasmonic Modulation of the Upconversion Fluorescence in NaYF₄:Yb/Tm Hexaplate Nanocrystals Using Gold Nanoparticles or Nanoshells. *Angewandte Chemie-International Edition*. 2010; 49(16):2865-2868.
- Zhang H, Xu D, Huang Y, and Duan XF. Highly spectral dependent enhancement of upconversion emission with sputtered gold island films. *Chemical Communications*. 2011; 47(3): 979-981.